

## **APPENDIX C. SEDIMENT TRANSFORMATION NUMERICAL MODELING INFORMATION**

## **C1. Hydrodynamic and Sediment Transport Results at Sand Resource Areas 1, 2, and 3**

Presented in this appendix are seasonal and extreme hydrodynamic and sediment transport results for the offshore Alabama resource areas, including potential borrow sites one, two, and three (four was presented and discussed in the main text, and it is not repeated here). Each figure includes maximum wave-induced velocities and directions, steady near bottom velocities and directions, initiation potential, and sediment transport rates and directions.

The resource area is affected by a combination of wave-induced bottom currents and steady near bottom currents. In turn these hydrodynamic processes may cause sediment transport. The extreme, or storm, cases at each resource area cause much more transport than the seasonally-averaged results. Storms are large initiators and movers of sediment given their large wave heights and long periods. Tables 5-4 and 5-5 in the main text present extreme and “average” results.

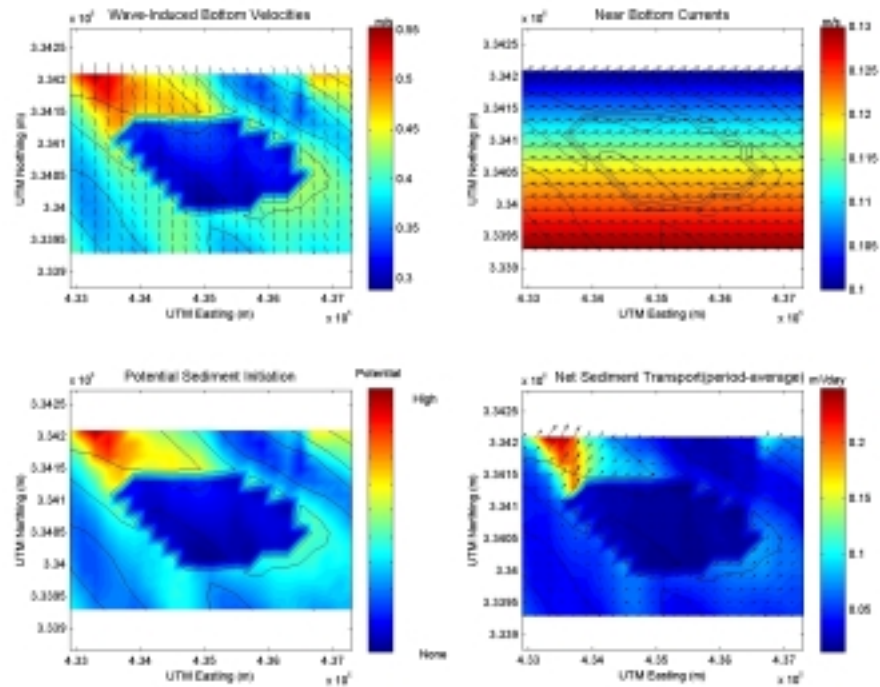


Figure C1-1. Northeast winter hydrodynamic and sediment transport results at Sand Resource Area 1. The solid black lines represent depth contours, and sediment transport results are based on 200 m cell widths.

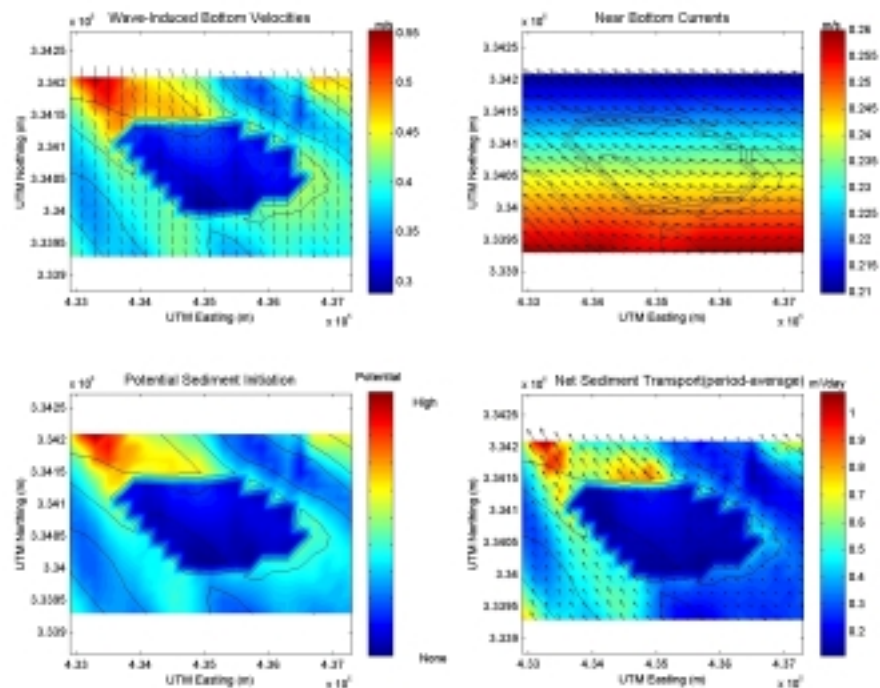


Figure C1-2. West winter hydrodynamic and sediment transport results at Sand Resource Area 1. The solid black lines represent depth contours, and sediment transport results are based on 200 m cell widths.

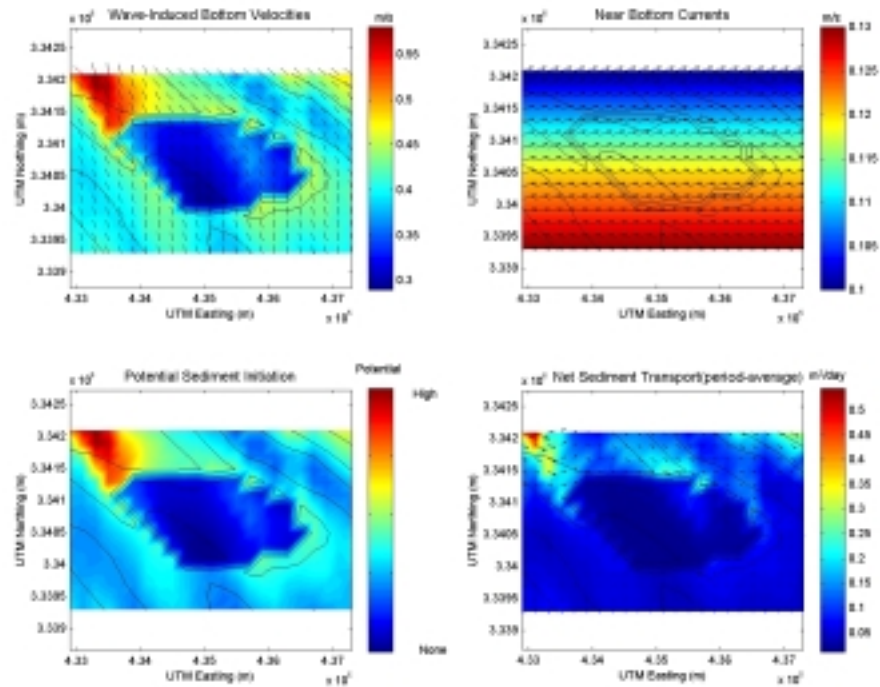


Figure C1-3. Spring hydrodynamic and sediment transport results at Sand Resource Area 1. The solid black lines represent depth contours, and sediment transport results are based on 200 m cell widths.

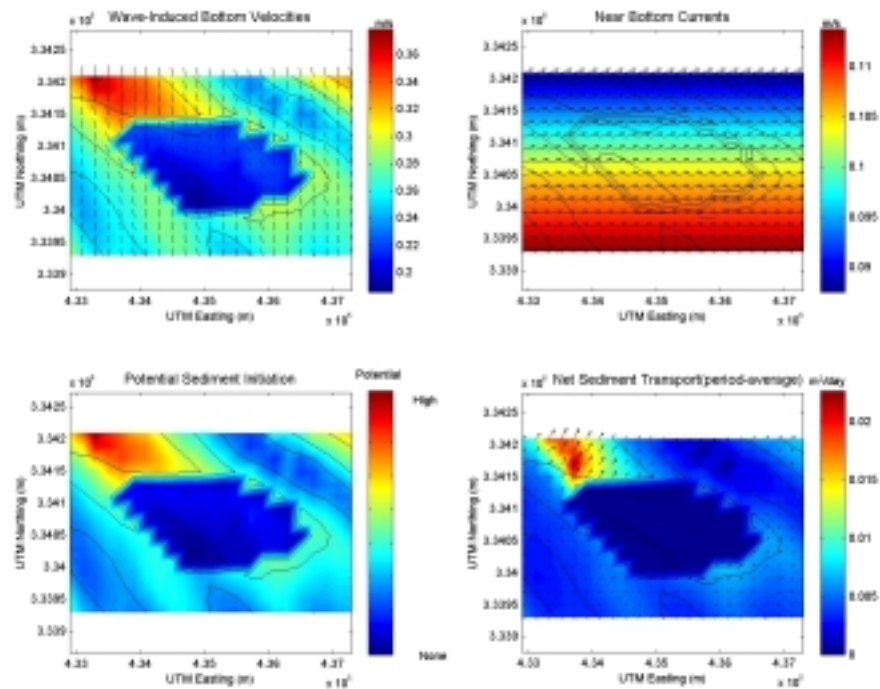


Figure C1-4. Summer hydrodynamic and sediment transport results at Sand Resource Area 1. The solid black lines represent depth contours, and sediment transport results are based on 200 m cell widths.

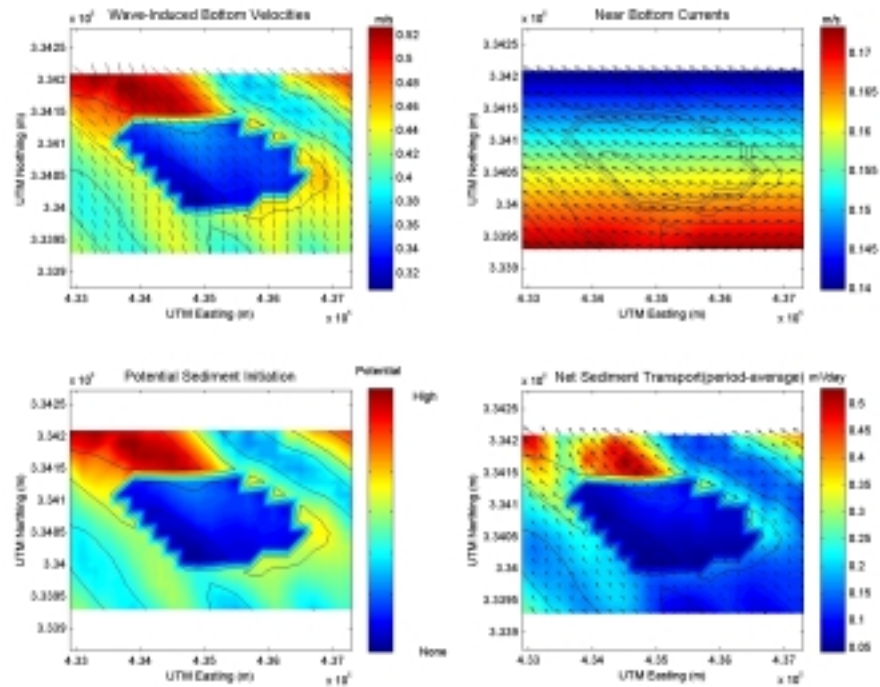


Figure C1-5. Fall hydrodynamic and sediment transport results at Sand Resource Area 1. The solid black lines represent depth contours, and sediment transport results are based on 200 m cell widths.

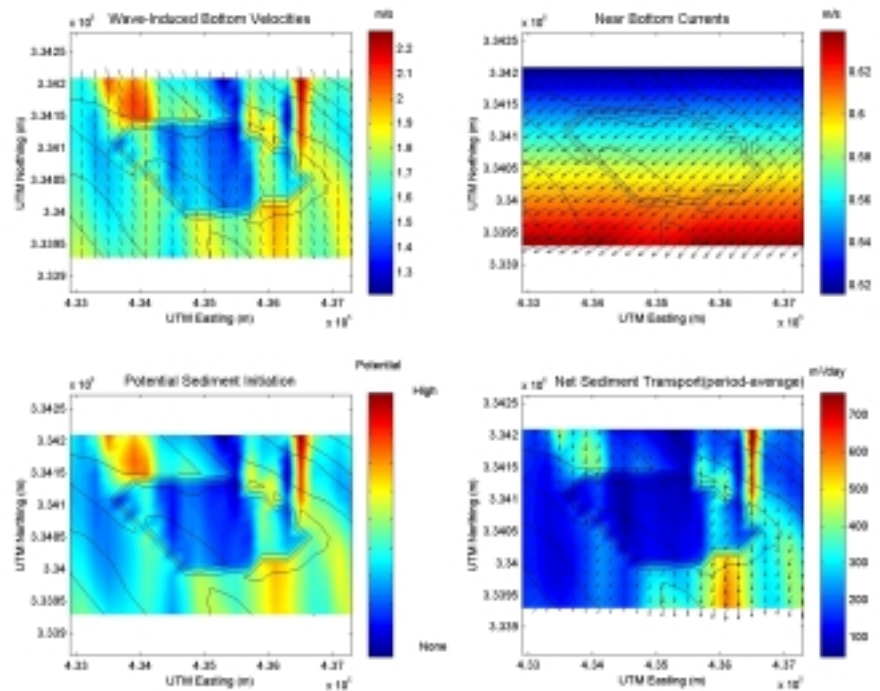


Figure C1-6. Storm hydrodynamic and sediment transport results at Sand Resource Area 1. The solid black lines represent depth contours, and sediment transport results are based on 200 m cell widths.

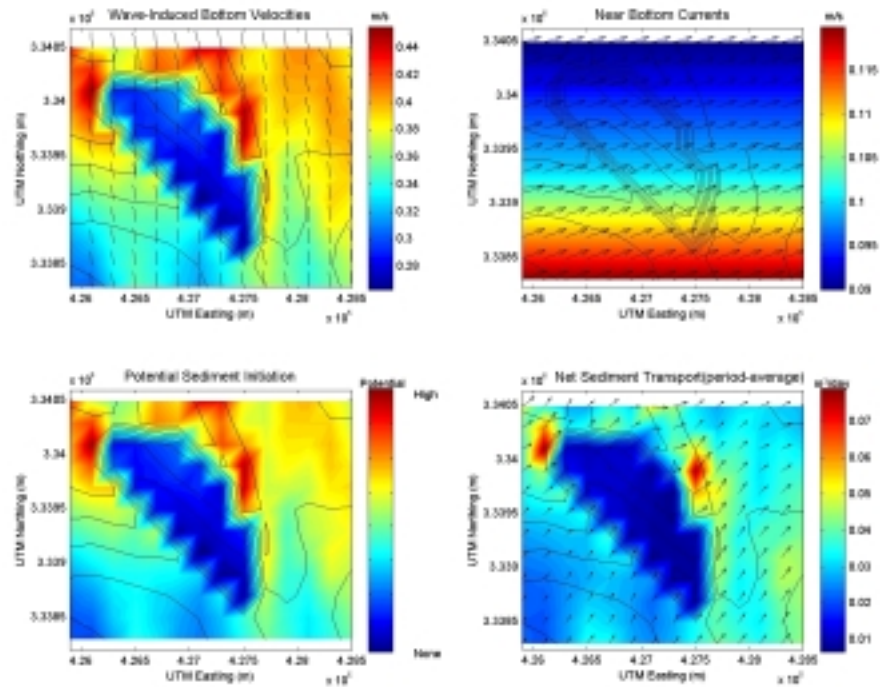


Figure C1-7. Northeast winter hydrodynamic and sediment transport results at Sand Resource Area 2. The solid black lines represent depth contours, and sediment transport results are based on 200 m cell widths.

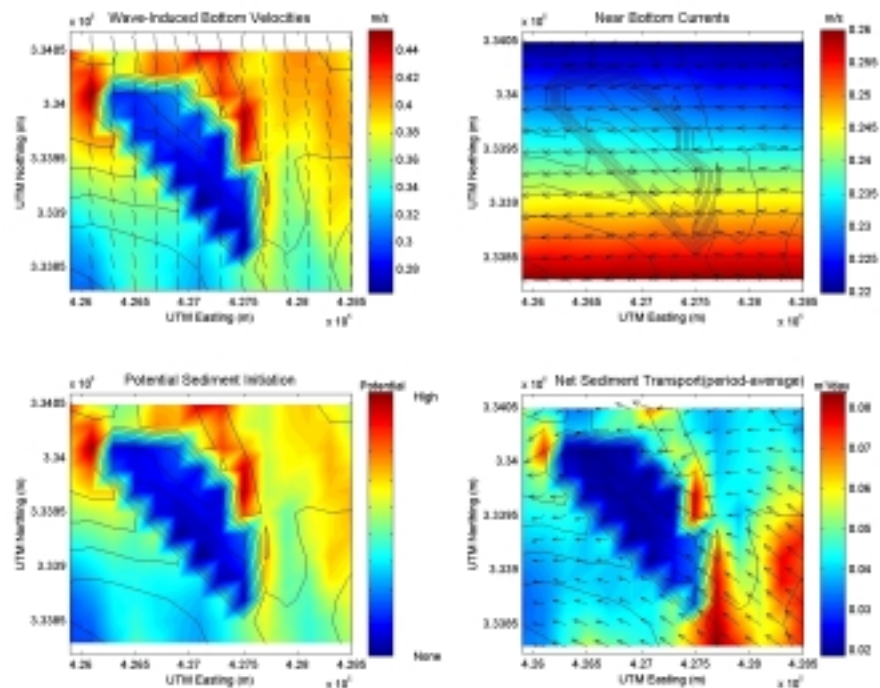


Figure C1-8. West winter hydrodynamic and sediment transport results at Sand Resource Area 2. The solid black lines represent depth contours, and sediment transport results are based on 200 m cell widths.

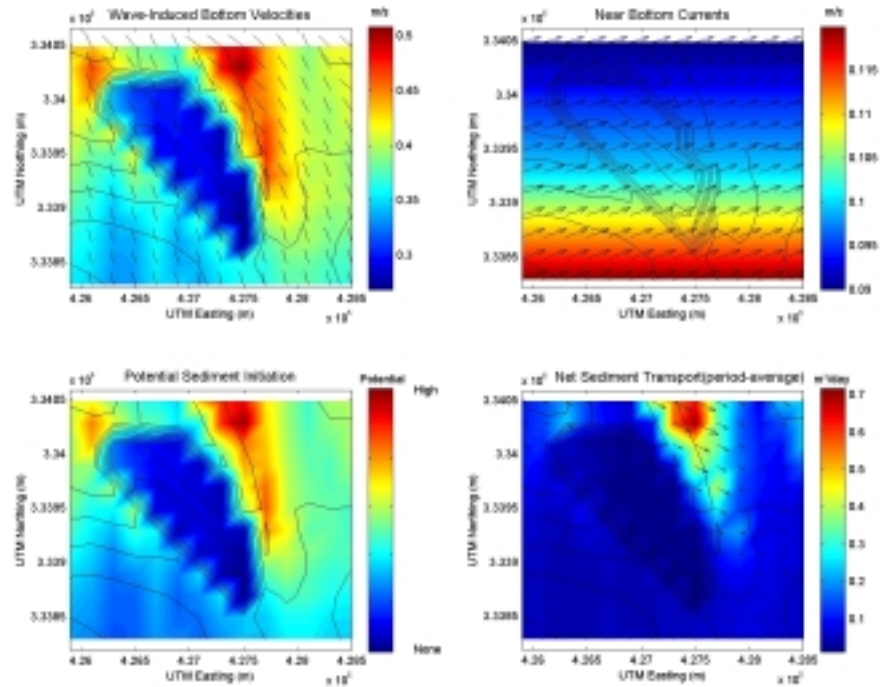


Figure C1-9. Spring hydrodynamic and sediment transport results at Sand Resource Area 2. The solid black lines represent depth contours, and sediment transport results are based on 200 m cell widths.

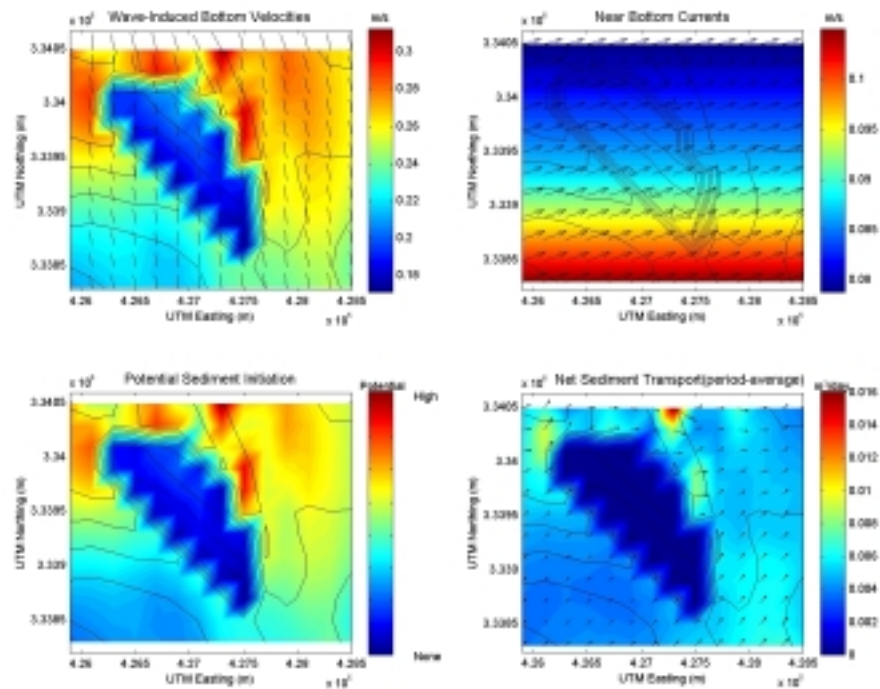


Figure C1-10. Summer hydrodynamic and sediment transport results at Sand Resource Area 2. The solid black lines represent depth contours, and sediment transport results are based on 200 m cell widths.

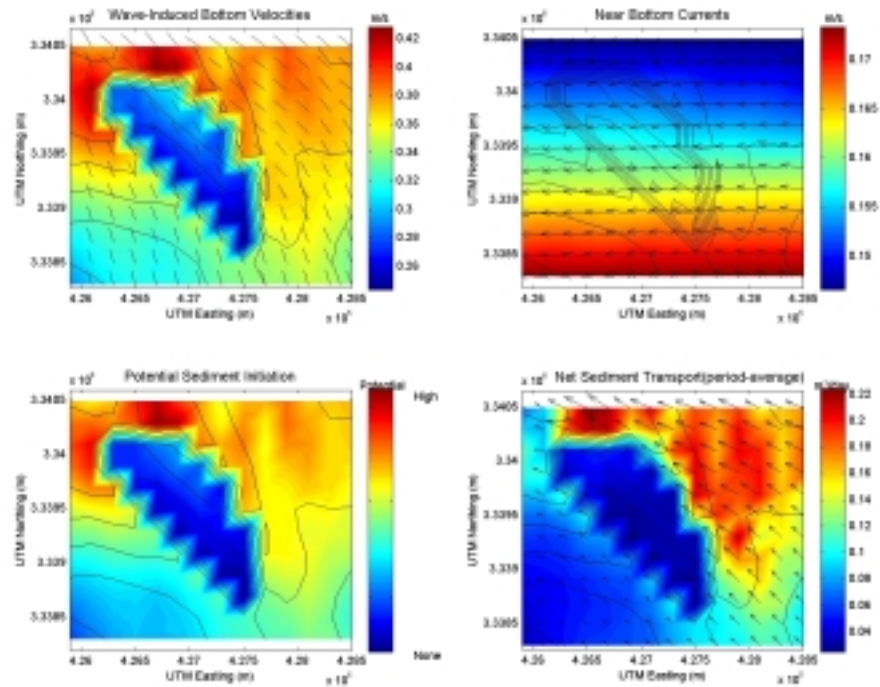


Figure C1-11. Fall hydrodynamic and sediment transport results at Sand Resource Area 2. The solid black lines represent depth contours, and sediment transport results are based on 200 m cell widths.

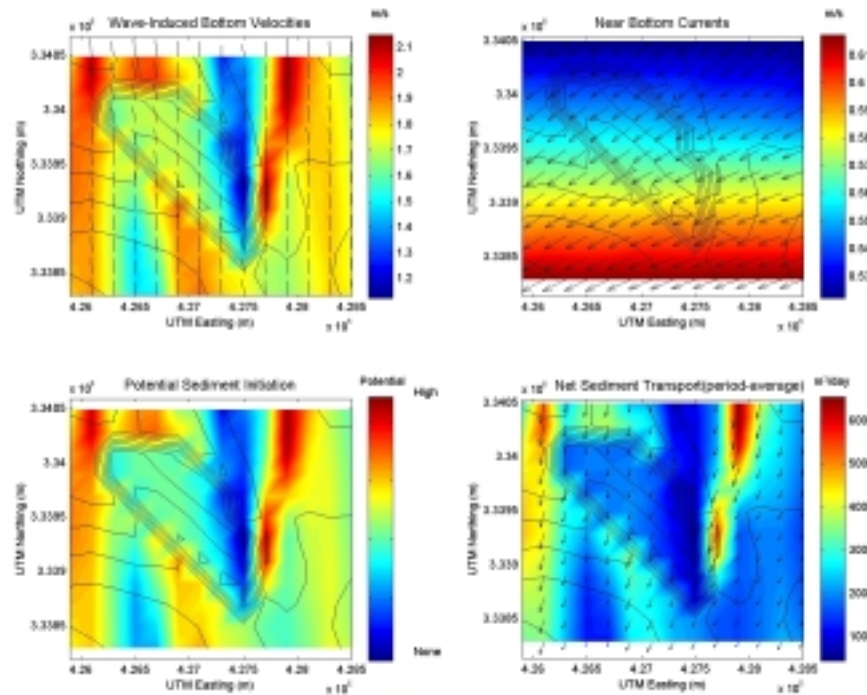


Figure C1-12. Storm hydrodynamic and sediment transport results at Sand Resource Area 2. The solid black lines represent depth contours, and sediment transport results are based on 200 m cell widths.

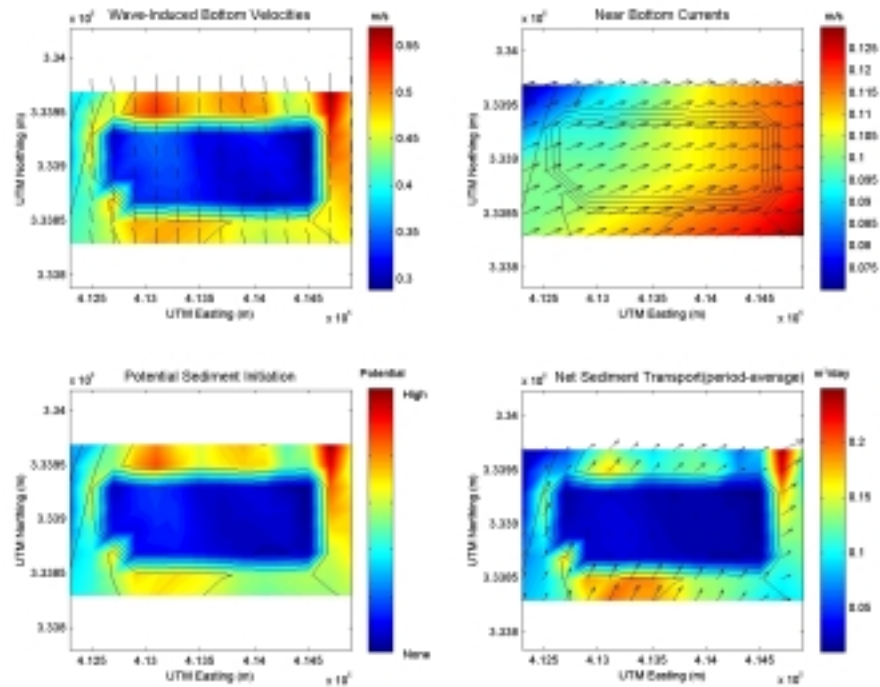


Figure C1-13. Northeast winter hydrodynamic and sediment transport results at Sand Resource Area 3. The solid black lines represent depth contours, and sediment transport results are based on 200 m cell widths.

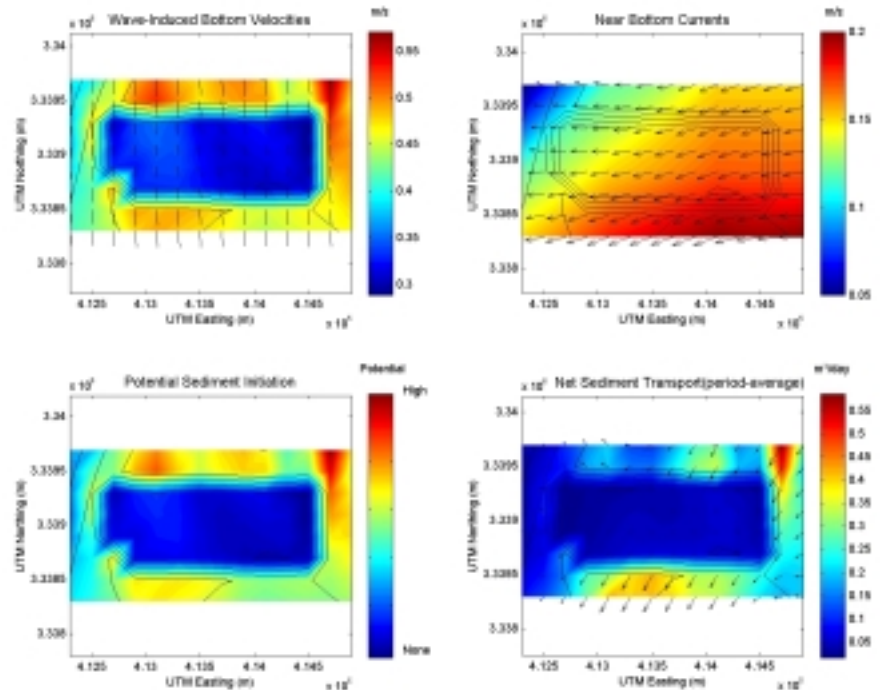


Figure C1-14. West winter hydrodynamic and sediment transport results at Sand Resource Area 3. The solid black lines represent depth contours, and sediment transport results are based on 200 m cell widths.

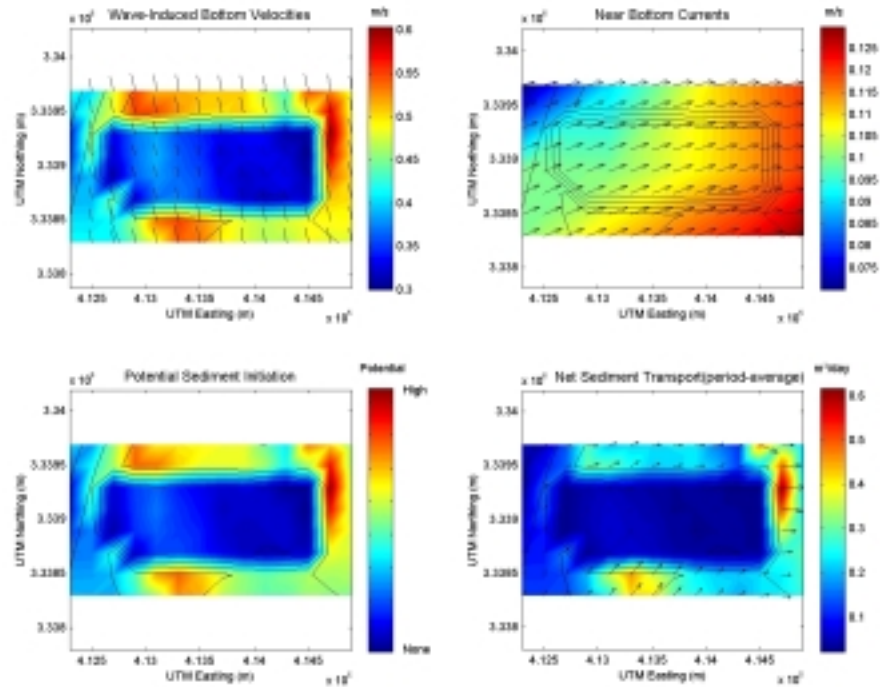


Figure C1-15. Spring hydrodynamic and sediment transport results at Sand Resource Area 3. The solid black lines represent depth contours, and sediment transport results are based on 200 m cell widths.

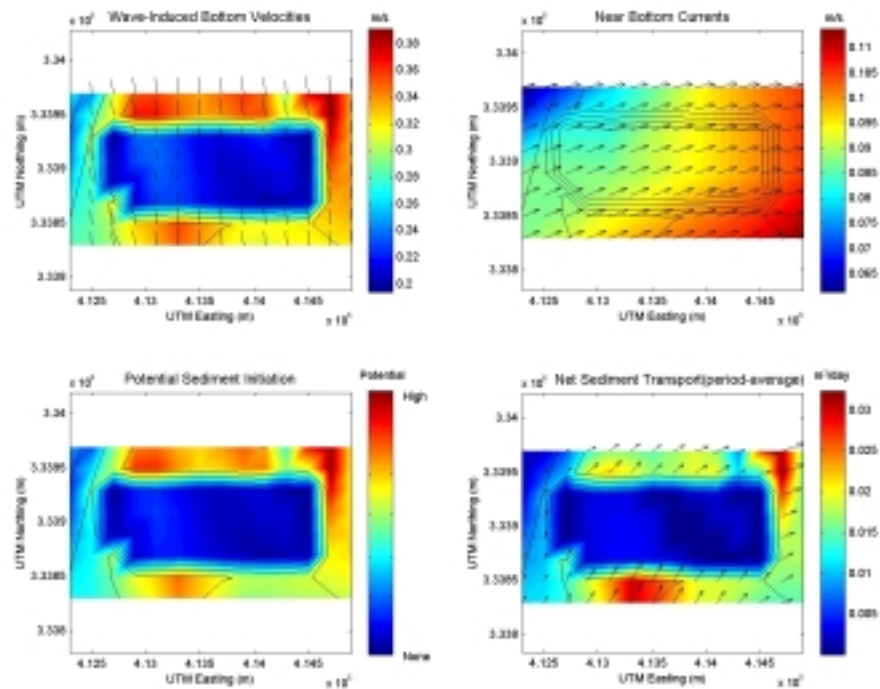


Figure C1-16. Summer hydrodynamic and sediment transport results at Sand Resource Area 3. The solid black lines represent depth contours, and sediment transport results are based on 200 m cell widths.

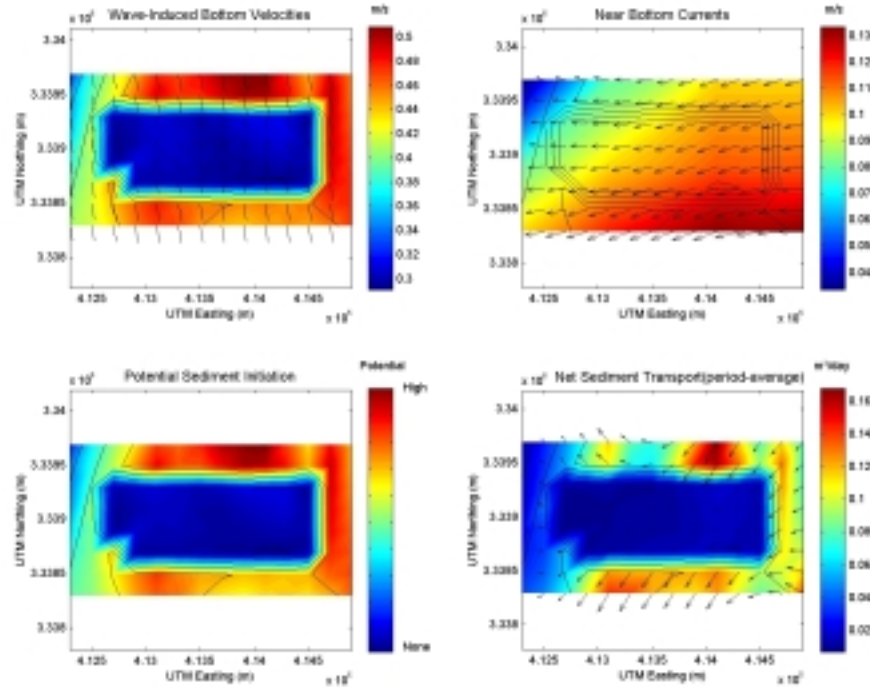


Figure C1-17. Fall hydrodynamic and sediment transport results at Sand Resource Area 3. The solid black lines represent depth contours, and sediment transport results are based on 200 m cell widths.

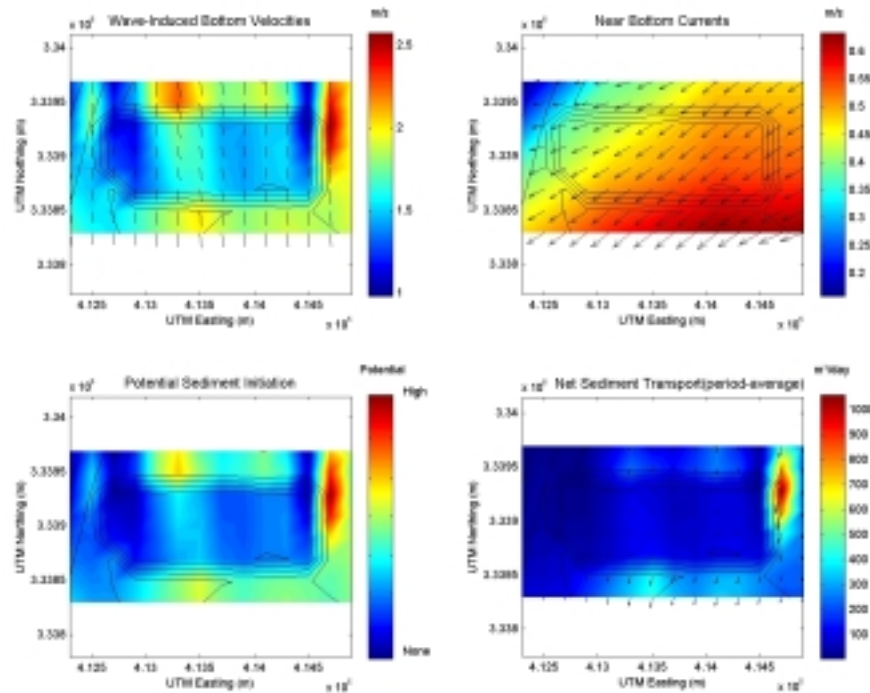


Figure C1-18. Storm hydrodynamic and sediment transport results at Sand Resource Area 3. The solid black lines represent depth contours, and sediment transport results are based on 200 m cell widths.

## C2. Longshore Sediment Transport Model Results

The following 20 plots provide  $S_{xy}$  radiation stress values as well as annualized longshore sediment transport rates. The radiation stress variation indicates the relative strength of longshore sediment transport potential. By plotting the nearshore variability of this quantity, areas of increased wave energy focusing can be determined. As expected areas of high radiation stress correspond to areas of high longshore sediment transport rate.

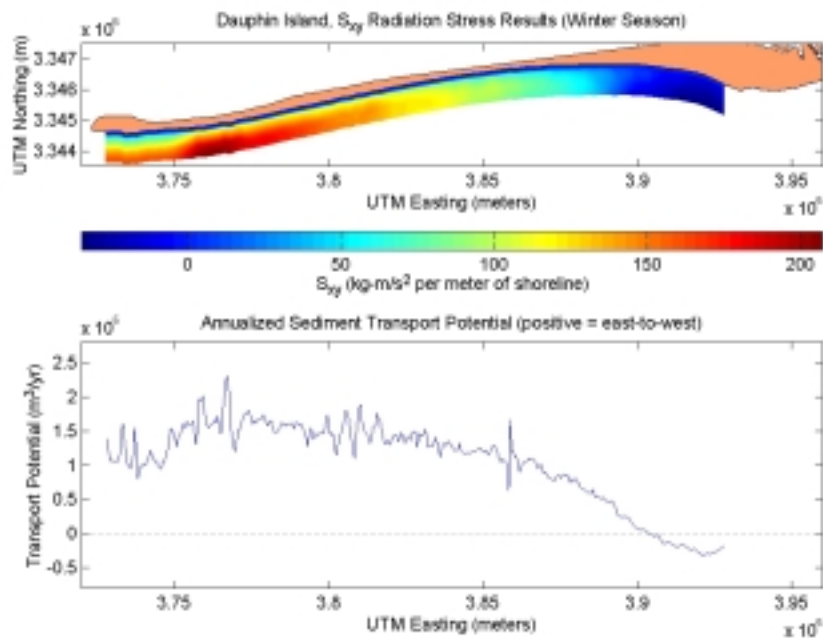


Figure C2-1.  $S_{xy}$  radiation stress and annualized sediment transport potential for existing conditions at Dauphin Island during the winter season.

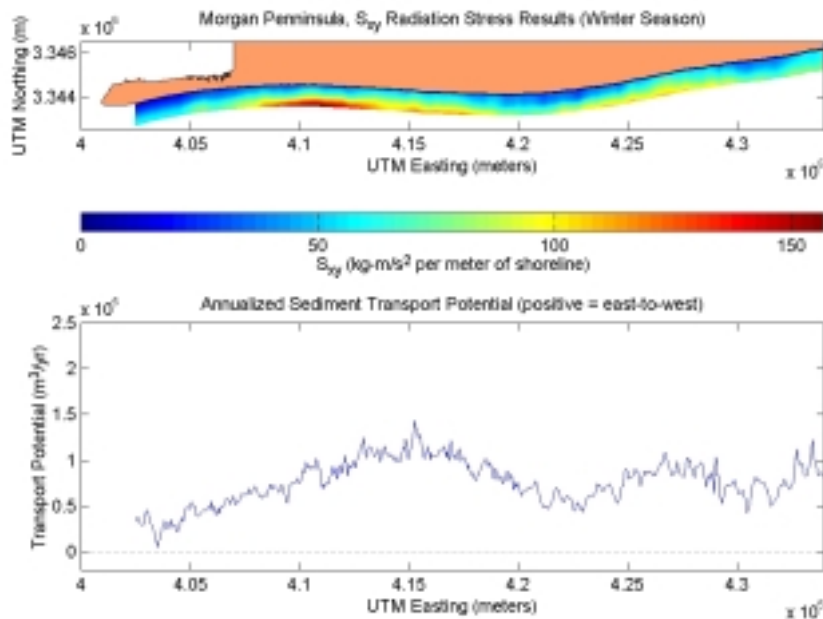


Figure C2-2.  $S_{xy}$  radiation stress and annualized sediment transport potential for existing conditions at Morgan Peninsula during the winter season.

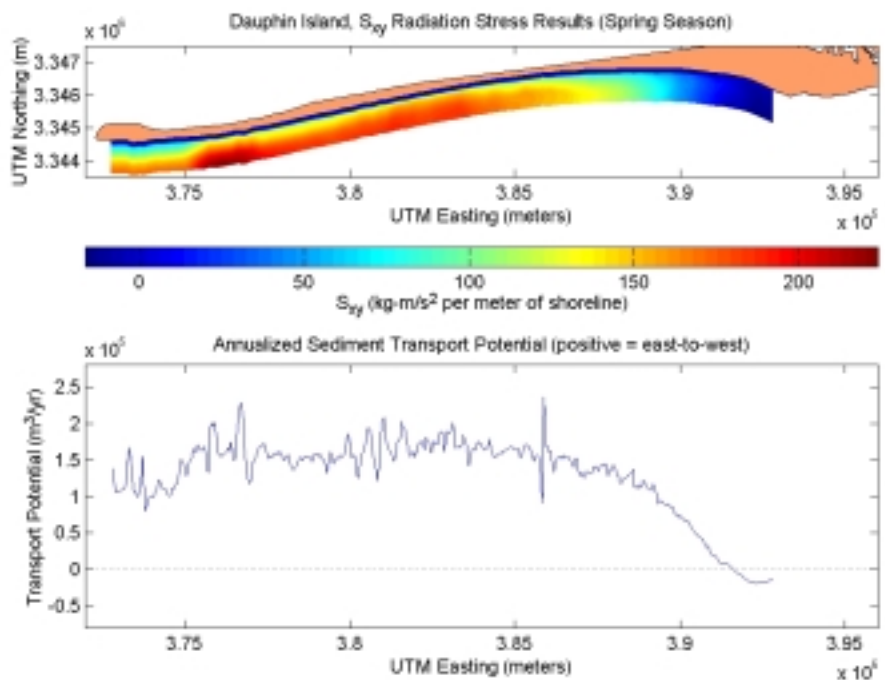


Figure C2-3.  $S_{xy}$  radiation stress and annualized sediment transport potential for existing conditions at Dauphin Island during the spring season.

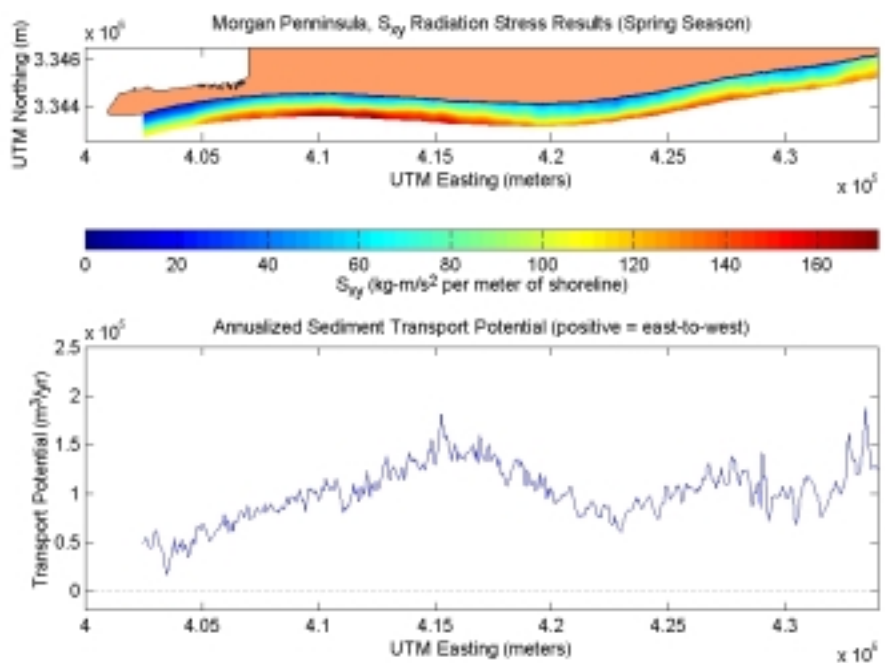


Figure C2-4.  $S_{xy}$  radiation stress and annualized sediment transport potential for existing conditions at Morgan Peninsula during the spring season.

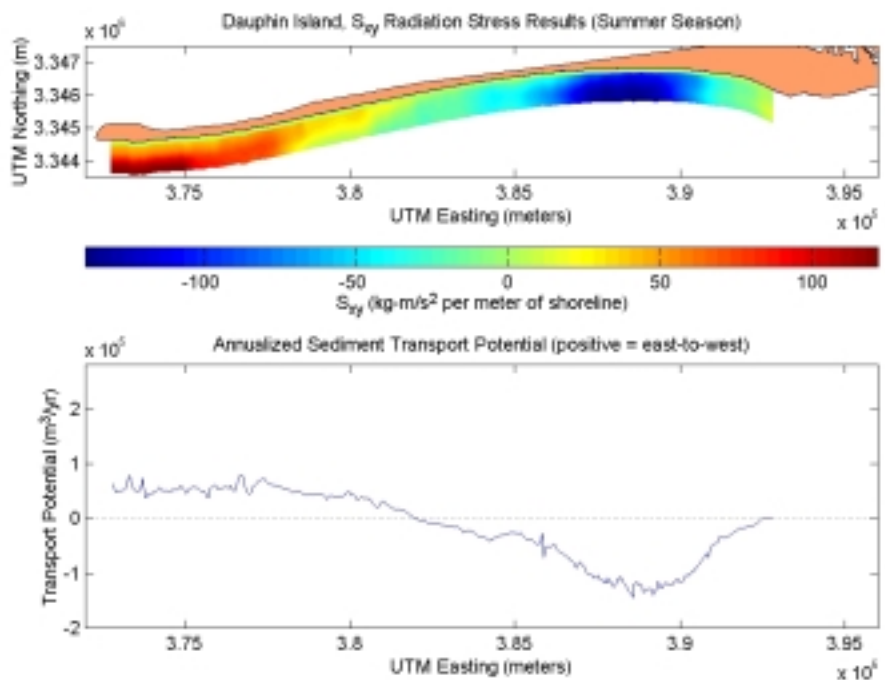


Figure C2-5.  $S_{xy}$  radiation stress and annualized sediment transport potential for existing conditions at Dauphin Island during the summer season.

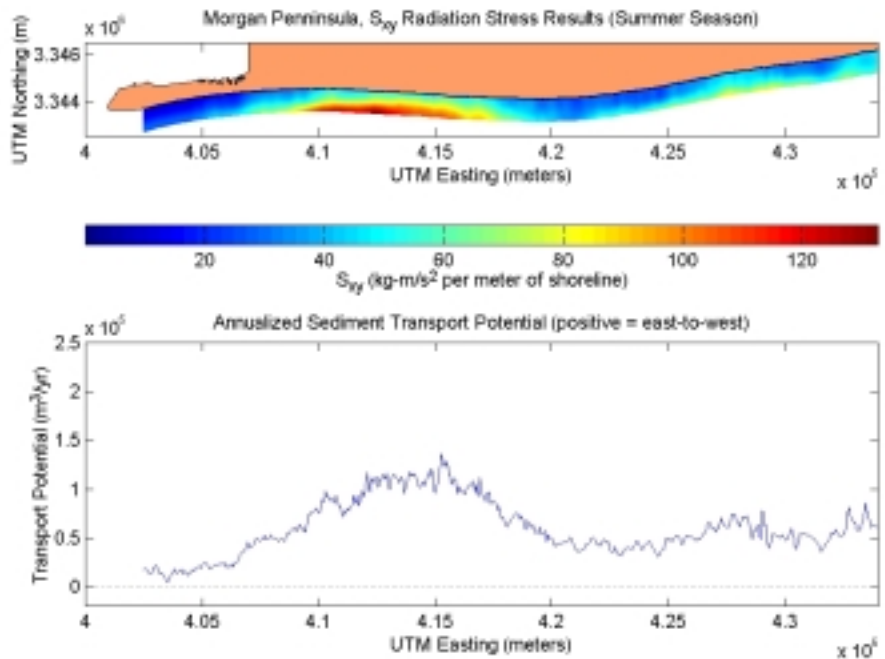


Figure C2-6.  $S_{xy}$  radiation stress and annualized sediment transport potential for existing conditions at Morgan Peninsula during the summer season.

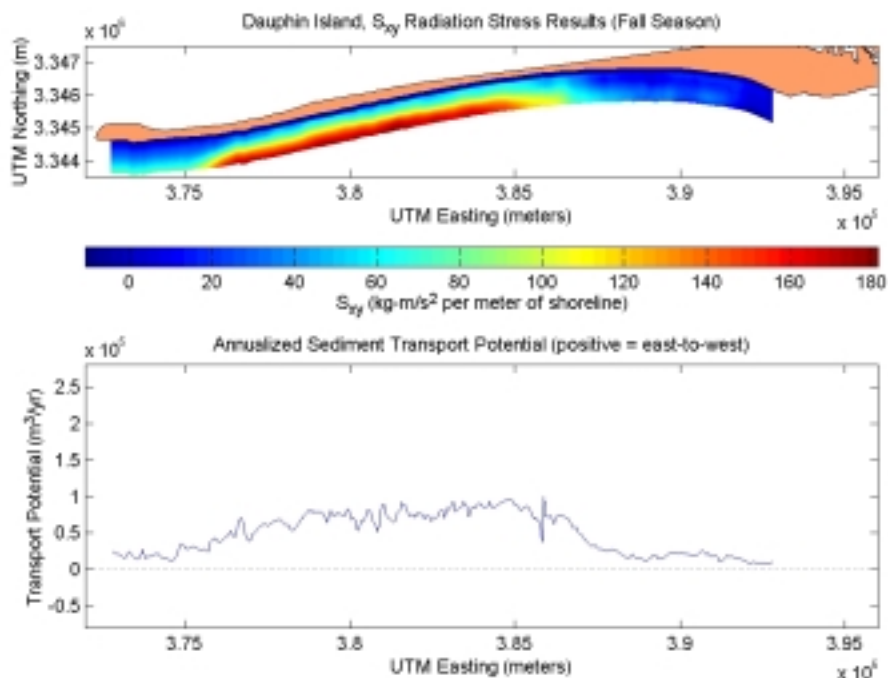


Figure C2-7.  $S_{xy}$  radiation stress and annualized sediment transport potential for existing conditions at Dauphin Island during the fall season.

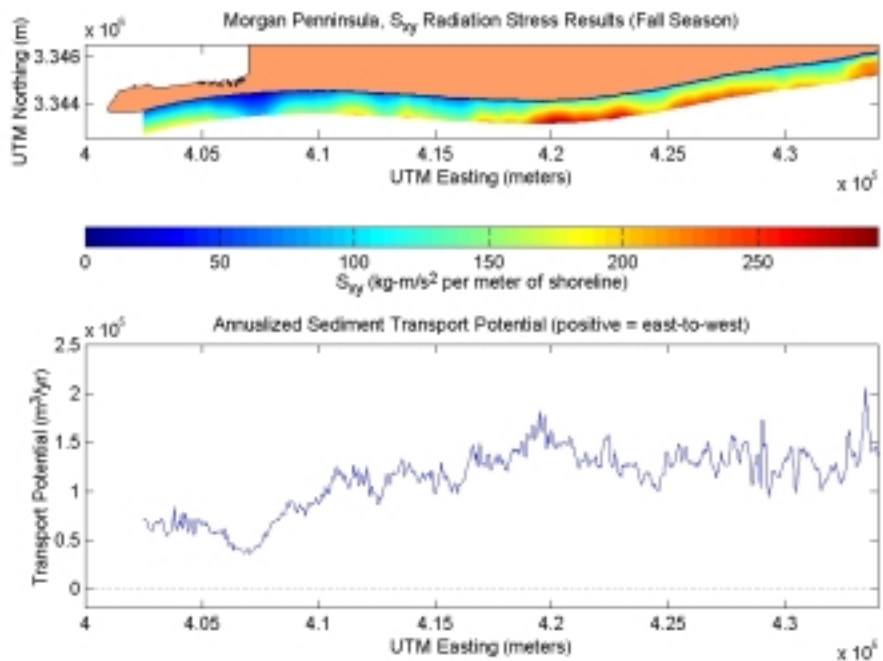


Figure C2-8.  $S_{xy}$  radiation stress and annualized sediment transport potential for existing conditions at Morgan Peninsula during the fall season.

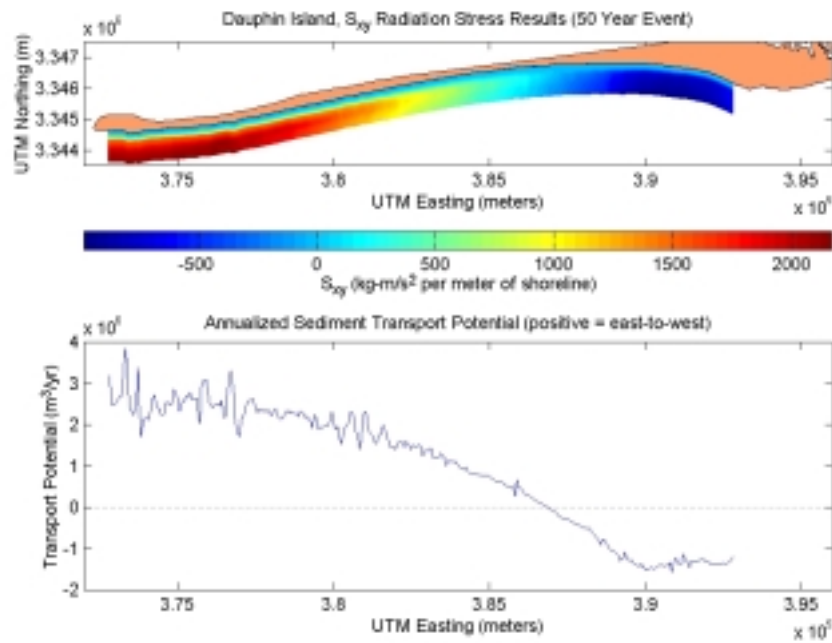


Figure C2-9.  $S_{xy}$  radiation stress and annualized sediment transport potential for existing conditions at Dauphin Island during a 50-year storm.

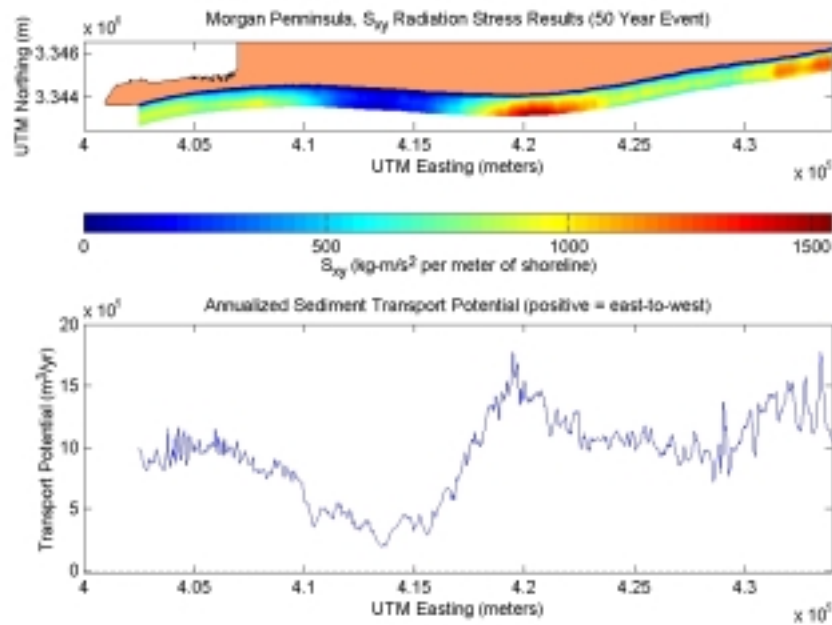


Figure C2-10.  $S_{xy}$  radiation stress and annualized sediment transport potential for existing conditions at Morgan Peninsula during a 50-year storm.

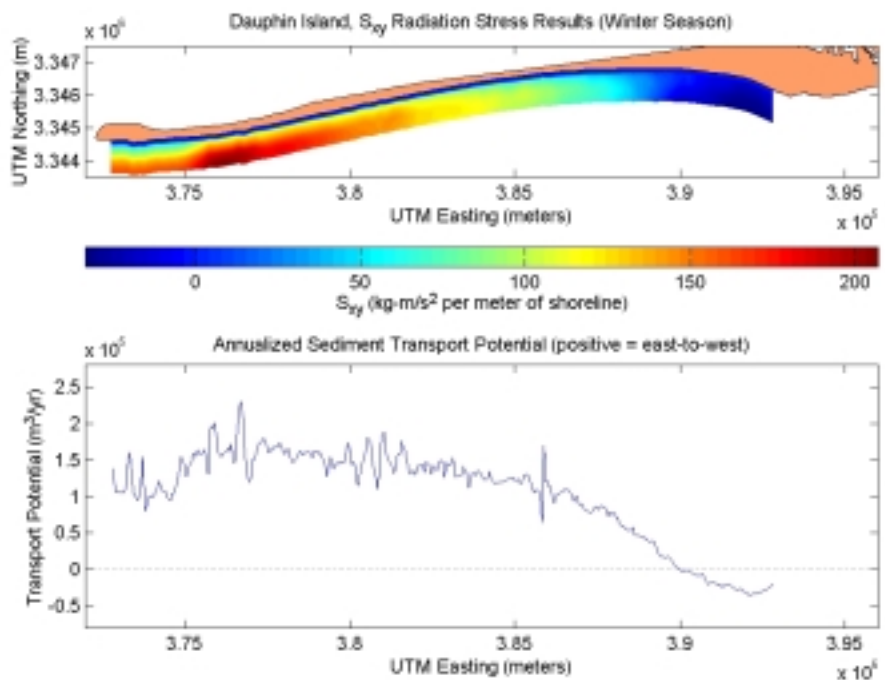


Figure C2-11.  $S_{xy}$  radiation stress and annualized sediment transport potential for post-dredging scenario at Dauphin Island during the winter season.

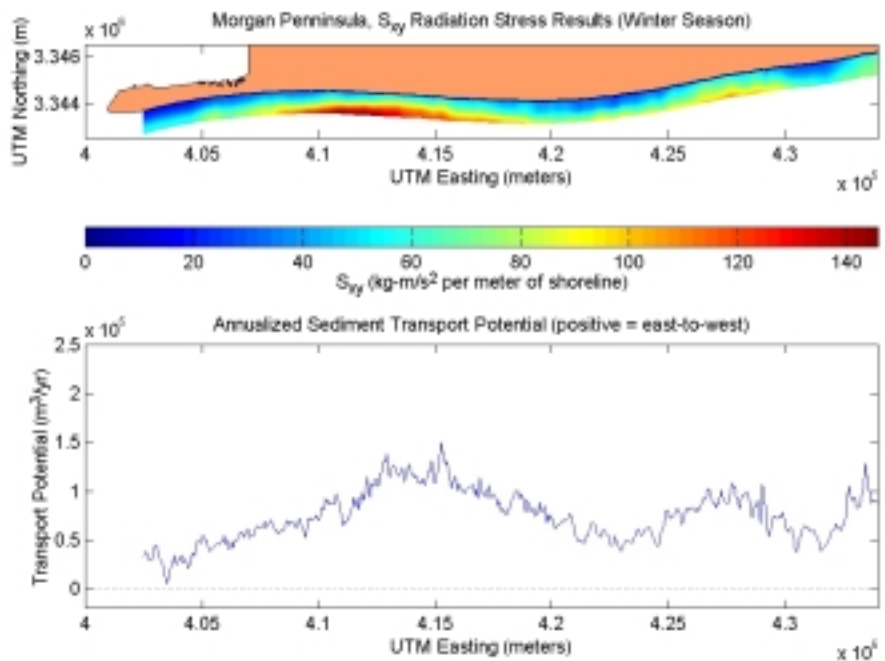


Figure C2-12.  $S_{xy}$  radiation stress and annualized sediment transport potential for post-dredging scenario at Morgan Peninsula during the winter season.

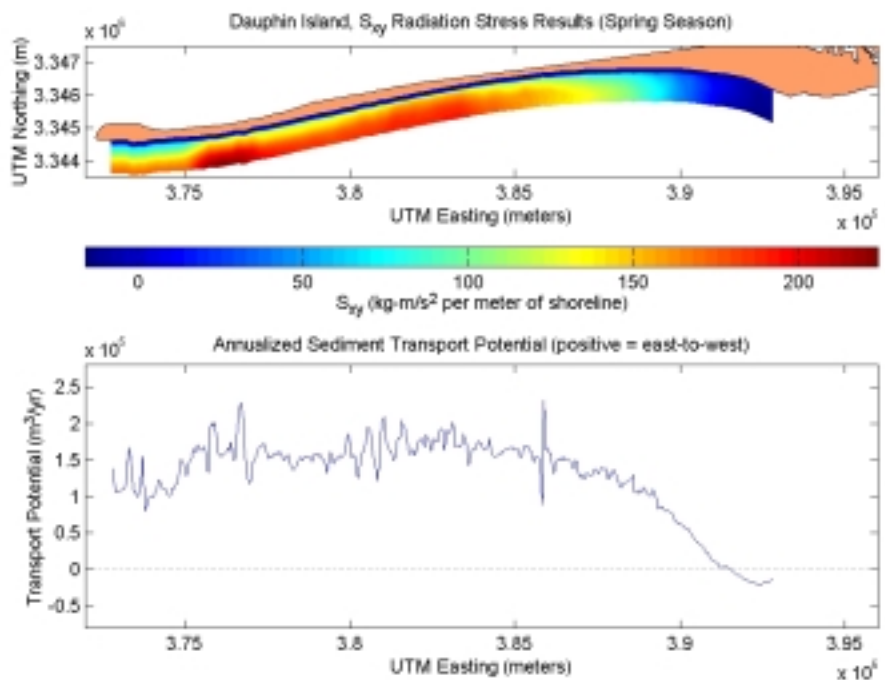


Figure C2-13.  $S_{xy}$  radiation stress and annualized sediment transport potential for post-dredging scenario at Dauphin Island during the spring season.

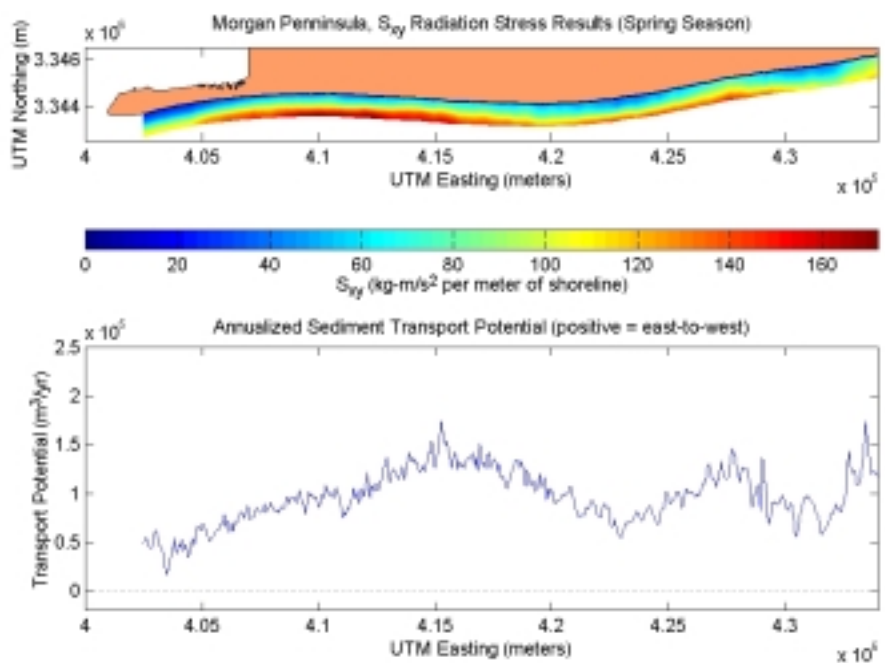


Figure C2-14.  $S_{xy}$  radiation stress and annualized sediment transport potential for post-dredging scenario at Morgan Peninsula during the spring season.

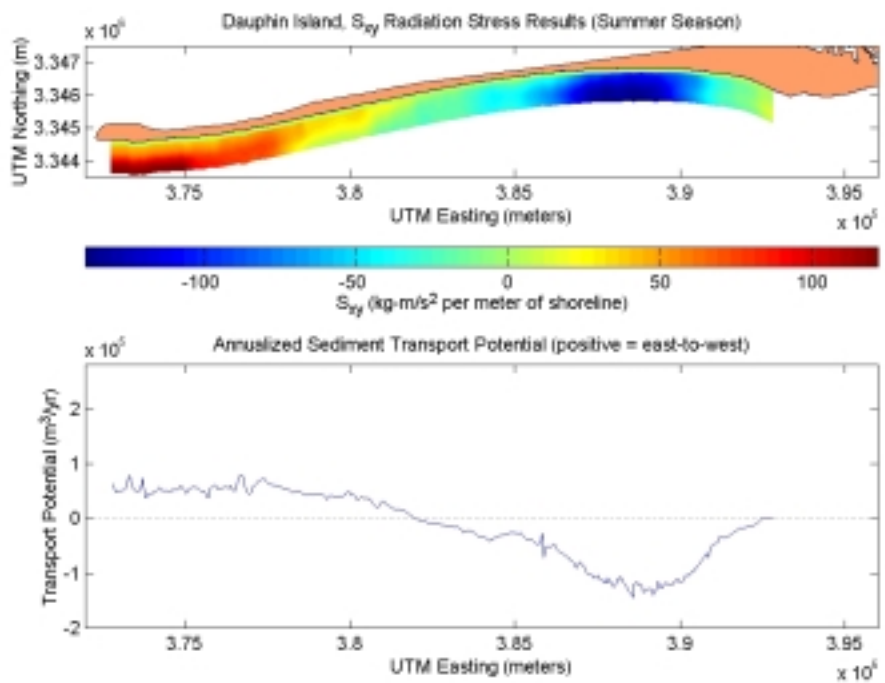


Figure C2-15.  $S_{xy}$  radiation stress and annualized sediment transport potential for post-dredging scenario at Dauphin Island during the summer season.

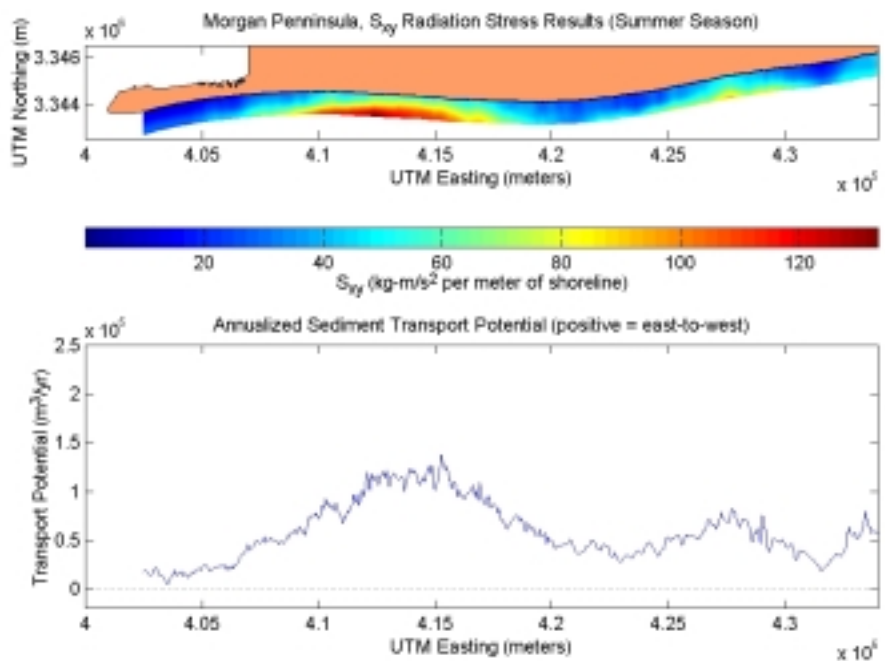


Figure C2-16.  $S_{xy}$  radiation stress and annualized sediment transport potential for post-dredging scenario at Morgan Peninsula during the summer season.

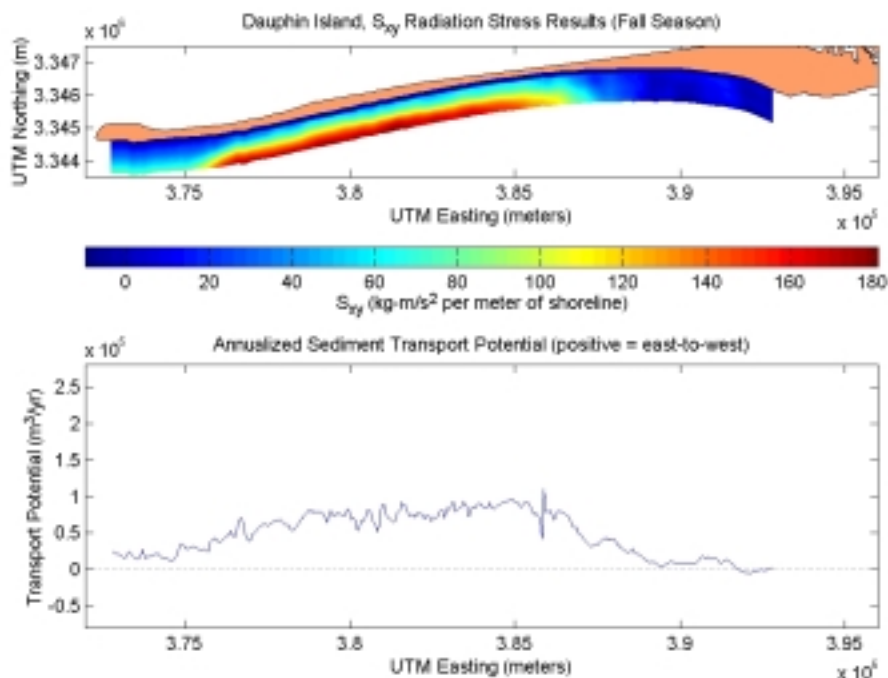


Figure C2-17.  $S_{xy}$  radiation stress and annualized sediment transport potential for post-dredging scenario at Dauphin Island during the fall season.

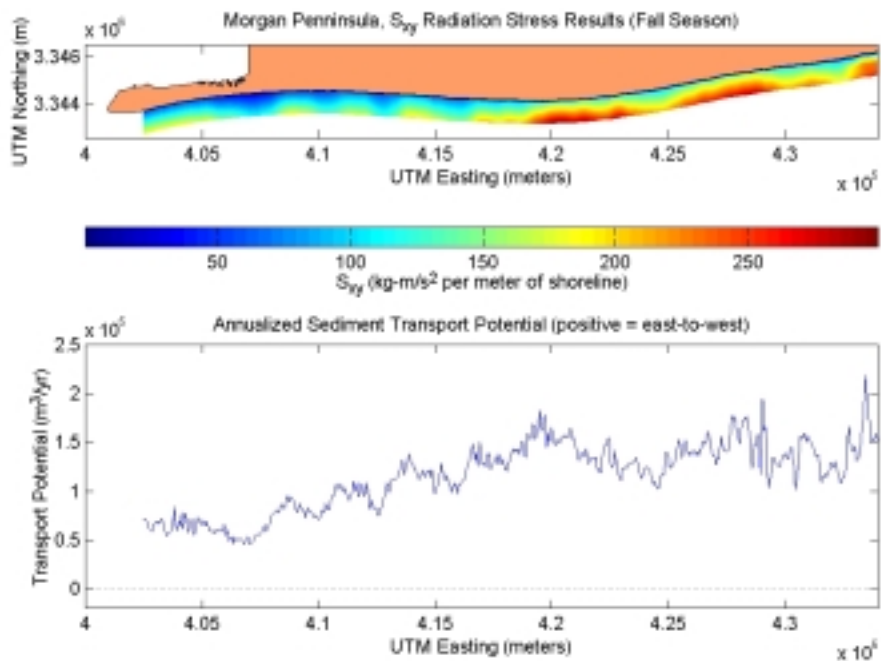


Figure C2-18.  $S_{xy}$  radiation stress and annualized sediment transport potential for post-dredging scenario at Morgan Peninsula during the fall season.

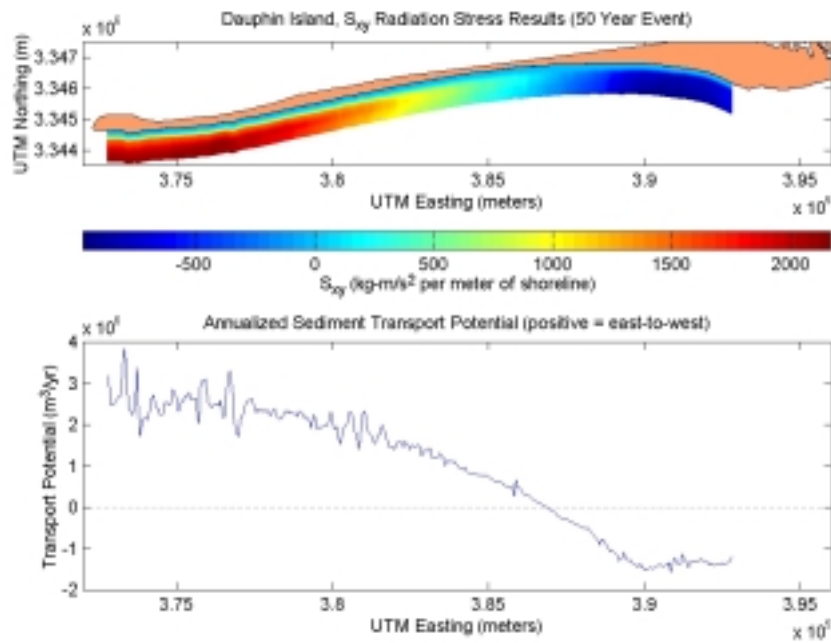


Figure C2-19.  $S_{xy}$  radiation stress and annualized sediment transport potential for post-dredging scenario at Dauphin Island during a 50-year storm.

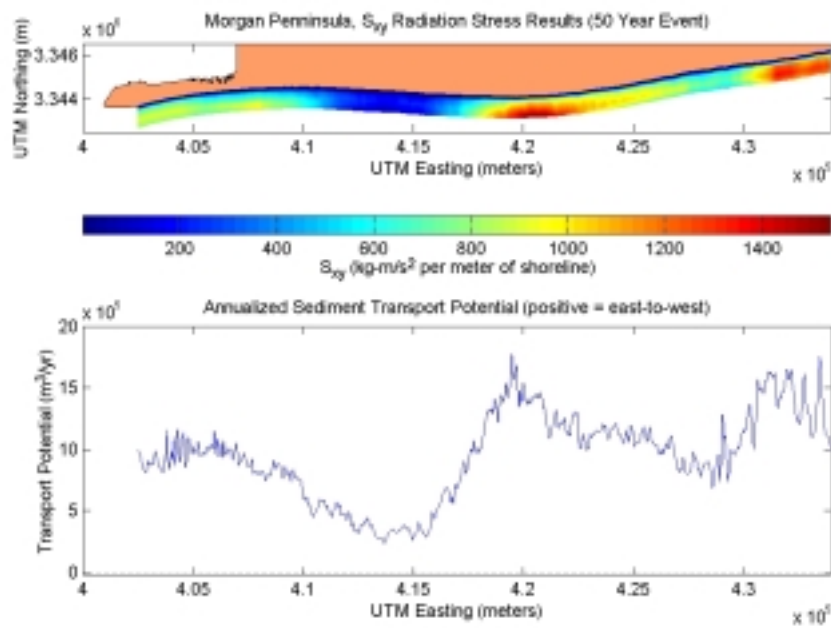


Figure C2-20.  $S_{xy}$  radiation stress and annualized sediment transport potential for post-dredging scenario at Morgan Peninsula during a 50-year storm.